AIMS Biophysics

AIMS Biophysics, 7(1): 1–16.
DOI: 10.3934/biophy.2020001
Received: 01 November 2019
Accepted: 31 January 2020
Published: 06 February 2020

http://www.aimspress.com/journal/biophysics

Research article

Peptide AEDL alters chromatin conformation via histone binding

Larisa I. Fedoreyeva[1,2]*, Boris F. Vanyushin[1,2] and Ekaterina N. Baranova[2]

[1] A.N.Belozersky Institute of Physico-Chemical Biology, Lomonosov Moscow State University, 119991 Moscow, Leninskie Gory1, building 40
[2] All-Russian Research Institute of Agricultural Biotechnology RAS, 127550 Moscow, Timiryazevskaya 42
* **Correspondence:** Email: fedlara@inbox.ru; Tel: +74999775263.

Abstract: Eukaryotic DNA is tightly packed into chromatin, a DNA–protein structure that exists as transcriptionally permissive euchromatin or repressive heterochromatin. Post-translational modification of histones plays a key role in regulating chromatin dynamics. Short peptides derived from various sources are known to function as epigenetic modulators; however, their mechanisms of action are poorly understood. We addressed this issued by investigating the effect of peptide AEDL on chromatin structure in tobacco (Nicotiana tabacum L.), a commercially important plant species. The chromatin of tobacco interphase cells is characterized by the presence of zones of transcriptionally active domains and particular domains of condensed chromatin of cells that partially coincide with heterochromatin zones. Chromatin decondensation and the formation of euchromatin, accompanied by the activation of genes expression activity, are a determining factor in responses to stressful effects. Our results show that plants grown in the presence of 10^{-7} M peptide AEDL transformed condensed chromatin domains from 45% in control cells to 25%. Histone modifications, which constitute the so-called histone code, play a decisive role in the control of chromatin structure. Fluorescence quenching experiments using fluorescein isothiocyanate-labeled histones revealed that the linker histone H1 and complexes of core H3 and H1 histones with DNA bound to peptide AEDL in a 1: 1 molar ratio. The peptide was found to bind to the N-terminal lysine residue of H1 and the lysine residue at position 36 of the H3 C terminus. These interactions of histones H1 and H3 with AEDL peptide loosened the tightly packed chromatin structure, getting transcriptionally active euchromatin. Our findings provide novel insight into the mechanism of gene regulation by short peptides and have implications for breeding more resistant or productive varieties of tobacco and other crops.

Keywords: chromatin transformation; ultrastructure; peptide-histone interaction

1. Introduction

Eukaryotic DNA forms a tightly packed structure known as chromatin that is important for the temporal and spatial regulation of gene expression [1]. The main unit of chromatin is the nucleosome, which is a repeating unit of 147 bp of DNA wrapped around an octamer comprising a histone heterotetramer (H3/H4) and two histone heterodimers (H2A/H2B). The positively charged histone proteins electrostatically interact with the negatively charged DNA. Nucleosome units are connected via a short DNA linker that associates with histone H1, which stabilizes the chromatin structure [2].

The transcriptionally permissive euchromatin and repressive heterochromatin states of chromatin are governed by combinations of post-translational covalent modifications of histones, including phosphorylation, acetylation, ubiquitination, ADP ribosylation, and methylation [3]. These modifications, which constitute the so-called histone code, are interdependent and create binding sites for chromatin-associated effector proteins that stimulate or limit transcription. The chromatin structure in eukaryotes is highly dynamic over the course of growth and development and changes in response to environmental factors. Chromatin remodeling controls basic molecular processes including gene transcription, replication, repair, and recombination [4,5]. DNA methylation and histone modifications are key mediators of epigenetic modifications. DNA methylation is usually associated with prolonged silencing of genes. Histone modifications lead to activation or repression of gene expression and can be removed after several cell cycles [6].

Euchromatin typically contain trimethylated histone H3K4 and highly acetylated histones H3 and H4. In contrast, histone H3 lysine 9 and/or 27 methylation is generally associated with gene silencing [7]. Histone methylation is catalyzed by members of family SET domain: the Suppressor of variegation SU(VAR)3–9, Enhancer of zeste E(Z), and Trithorax (TRX); and non-SET domain: Dot1/Dot1L, and arginine methyltransferase families [8]. Recent genome-wide profiling studies have shown that most genes contain methylated histones and that distinct methylation patterns are associated with different transcriptional states [9,10]. For example, actively transcribed genes often exhibit H3K4 and H3K36 monomethylation, whereas repressed genes are enriched in H3K27 trimethyl marks.

Nucleosomes connected by linker DNA form a 10-nm array resembling beads on a string. Linker histones further condense this linear structure into a 30-nm chromatin fiber, which requires interaction between the N-terminal tail of histone H4 and a specific surface region on the adjacent nucleosome known as the acid patch formed by the negatively charged residues Glu56, Glu61, Glu64, Asp90, Glu91, and Glu92 of H2A and Glu102 and Glu110 of H2B [11]. Some nucleosome-binding proteins specifically interact with the acid patch and may play a role in regulating higher-order chromatin structure by competing with the N-terminal tails of H4 for binding to this nucleosome region [12,13]. The diversity of these proteins in plants suggests that they have specific functions during development. For example, MEDEA in Arabidopsis is a polycomb group protein homologous to E(Z) that regulates seed development after fertilization [14]. The ATX1 protein, a homolog TRX, regulates the expression of several floral homeotic genes in Arabidopsis confirming it is histone H3K4 methyltransferase [15]. The protein product of the ASHH2 gene related to Drosophila absent, small, or homeotic discs 1 (ASH1) is involved in the control of flowering time and acts as a H3K4 and/or H3K36 histone methyltransferase [16].

Chromatin structure is affected by external stressors such as temperature, drought, high salt concentration, and infection. For example, viruses interact with condensed DNA; human

cytomegalovirus was shown to attach to condensed DNA when cells prepare to divide, and a 72-kDa viral protein was found to interact with the histone motif that is involved in nucleosome binding and chromatin condensation [17].

Peptides form a signal regulatory system that controls the growth and development of animals and plants [18]. Short exogenous peptides selectively modulate gene expression and protein synthesis, including those involved in DNA replication and repair and responsible for cell differentiation in animals [19]. In plants, as in animals, short peptides induce the expression of genes encoding transcription, cell differentiation, growth, and development factors [20]. The action of such peptides is gene-specific and, apparently, has an epigenetic nature.

It was previously shown that peptide AlaGluAspGly [21] induces the activation of ribosomal genes, the decondensation of closely packed chromatin fibrils, and the release of genes repressed as a result of age-related condensation of euchromatin cell domains. The ability AlaGluAspGly to activate heterochromatin in lymphocyte cells in senile patients has been established.

The aim of this study is that a peptide AlaGluAspLeu with a similar structure to peptide AlaGluAspGly is capable of decondensing tobacco plant chromatin.

2. Materials and Method

2.1. Tobacco seeds

Tobacco seeds (N. tabacum L., Samsun cultivar) were germinated in flasks with agarose hormone-free Murashige – Skooge medium (MS). The cotyledons formed after seed germination were placed in Petri dishes with agarose MS medium and MS medium containing peptide AlaGluAspLeu (10^{-7} M). Developing tobacco regenerants leaves from callus (of 3 weeks seedlings explants on MS with/and without synthetic peptide AEDL (10^{-7} M) were used in the experiments. The seeds were germinated in petri dishes (100 seeds per dish) on aqueous salt solutions. First, the seeds were kept in darkness for 24 h at 20–25 ℃, and then in darkness at 17–18 ℃ and under light with a 12-h photoperiod at 20–25 ℃.

2.2. Electron microscopy

Cotyledons and roots of 4- and 8-day-old seedlings were used for electron-microscopic analyses. The same seedling organs taken after 2, 4, and 8 days of germination on distilled water were used as the controls. Leave regenerants fragments about 0.5–1.0 mm in width and 1–2 mm in length, were used for routine electron microscopy procedure. They were fixed for 4 h at room temperature in a 2,5% solution of glutaraldehyde in 0.1 M Na-phosphate buffer, pH 7.2, containing sucrose (15 mg/ml). After two times washing in the same buffer we used the post fixation of the material with 1% osmium tetroxide was performed for 2 h. Later the material was dehydrated and embedded into Epoxide resin using a standard technique. Ultrathin sections were prepared with an LKB-III microtome (LKB, Sweden). The sections were stained with lead citrate and viewed under an H-500 transmission electron microscope (Hitachi, Japan) at an accelerating voltage of 10 kV and operating magnification of 10000 ×. For chromatin morphology statistical analyses we measured the area of the nucleus, its osmiophilic and bright areas. We use more than 30 photos of plant leaves nucleus from fragments of three different regenerants from callus with growing with or without AEDL.

2.3. The tetrapeptide AlaGluAspLeu

(AEDL) was synthesized at the St. Petersburg Institute of Bioregulation and Gerontology RAS. The purity of the synthetic peptides was checked by chromatography on a BioLogic DuoFlow chromatograph on a C-18 column in a concentration gradient of acetonitrile (0–60%) containing 1% trifluoroacetic acid.

2.4. Isolation and purification of histones

Histones were isolated from the fraction of cellular nuclei of tobacco regenerants. A nuclear fraction was obtained by extraction of the crushed tissue with 20 mM TEA buffer, pH 7.5, containing 0.4 M sucrose, 30 mM KCl, 5 mM $MgC1_2$, 10 mM EDTA and protease inhibitors (1 mM PMSF and 1 mM iodoacetate). The protein fraction was obtained by extraction from purified nuclei by precipitation of 0.74 M $HClO_4$. The total histone fraction was separated in 15% SDS-electrophoresis. Histones were isolated from the gel by electroelution. The protein concentration in the obtained preparations was determined by staining an aliquot on the membrane according to the calibration curve.

2.5. Labeled with fluorescein isothiocyanate

Fluorescein isothiocyanate (FITC) -protein preparations were obtained by adding a solution of FITC in 0.5 M sodium bicarbonate to a buffer solution of proteins in a ratio of 1.2 M: 1 M. The reaction mixture was kept at room temperature for 30 min with shaking [22]. Free FITC was removed on an Amicon 3000 membrane. The obtained fluorescently labeled proteins were analyzed by chromatography on a BioLogic DuoFlow chromatograph on a C-4 column in a concentration gradient of acetonitrile (0–100%) containing 1% trifluoroacetic acid. The efficiency of incorporation of a fluorescent label into proteins was determined by the absorption spectrum using the equation: [FITC-H] = $(A_{280} - 0.24\ A_{495})/\acute{\varepsilon}\ l$, where A is the absorption at a given wavelength, ε is the histone extinction coefficient equal to $4470M^{-1}\ cm^{-1}$ (under the assumption that the absorption spectrum of the protein itself does not significantly change upon modification), l is the optical path length [23]. A fluorescent label was incorporated into the proteins in an approximately 1: 1 molar ratio (0.8–1.2), and the fluorescent probe was localized at the N-terminal α-amino group of proteins [22].

2.6. DNA isolation

DNA from tobacco regenerants was isolated by a standard method using DNA isolation kits (DNA Extran, Syntol, Russia). The purity of the preparations was determined by electrophoresis in 1% agarose. Like The mass of the obtained DNA was determined relative to DNA markers. DNA concentration was determined spectrophotometrically.

2.7. The formation of histone-DNA complexes

The formation of protein-DNA complexes was carried out in a ratio of 1.0 M: 0.5 M, respectively, at 37 °C for 15 minutes. In the case of the formation of a complex of FITC-histones with DNA, the formation of the complex was used by the change in the fluorescence intensity.

2.8. Static quenching of fluorescence

Stern-Volmer equation Static quenching with complex formation can be described using the Stern-Volmer equation [24]: $F_o/F = 1 + K_q [Q]$, where F_o is the initial fluorescence intensity, F is the fluorescence intensity when a quencher is added, [Q]-quencher concentration, Kq-quenching constant or Stern-Volmer constant, defined as the angle of inclination of the line. Fluorescence spectra were recorded on a Perkin-Elmer LS 55 spectrofluorimeter (USA). Titration of FITC-labeled histones with peptides and FITC-labeled peptides with oligonucleotides of different methylation status was carried out with equal volumes of the peptide AEDL at 24 ℃ with stirring. Solutions with a fluoroprobe were excited with a wavelength of 413 nm and emission spectra were recorded from 480 nm to 600 nm. Fluorescence spectra were recorded 5 minutes after the addition of the peptide. These experiments were performed at least 3 times. Fluorescence intensities (F) were adjusted for dilution of enzyme solutions when peptide solutions were added. The value of the fluorescence quenching rate constants was calculated by the formula: kq = Ksv/τ, where τ = 5 ns is the average lifetime of a biomolecule without a quencher [25]. The obtained values of kq are 4–5 orders of magnitude higher than the maximum quenching rate constant in diffusion collisions of a large amount of a quencher with a biopolymer. Therefore, we can assume that at low concentrations [Q], the process of quenching of fluorescence is controlled by static quenching due to the formation of protein-peptide complexes, and not by a dynamic collision of molecules. To determine the binding constants, we used equation (1) and equation (2) - $\log [(F_0 - F)/F] = \log Kb + n \log [Q]$, where Kb and n are the constant and the number of binding sites. From equations (1) and (2), equation (3) is obtained -K sf = Kb [Q] n-1. For n = 1 Ksf = Kb. This allowed us to use the Stern-Volmer constant to evaluate the binding of peptides to various histones.

2.9. RNA

RNA was isolated from individual tobacco callus regenerants. RNA was isolated using the RNA-Extran reagent kit Synthol (Russia) according to the protocol. The concentration of the isolated preparations were determined spectrophotometrically on Nanophotometer Implen.

2.10. cDNA

cDNA was obtained by standard methods using a reagent kit (Synthol) for reverse transcription. Information on the primary structure of the histone methyltransferase genes of Nicotiana tabacum was taken from the NCBI database. Primers for these genes were selected using the online service NCBI Primer-BLAST and synthesized by Syntol (Table). Real-Time System thermal cycler (BioRad, USA). Samples were prepared by the standard method using a set of reagents for PCR-RT in the presence of SYBR Green I (Synthol). The PCR-RT reaction was carried out under identical conditions for all samples: 95 ℃–5 min, then 45 cycles–94 ℃–30 s, 58 ℃–30 s, 72 ℃–30 s. The reaction was carried out in 2–3 parallels and in three repetitions. The relative level of gene expression was calculated by a calibration curve constructed with PCR products obtained with primers for the *GaPDh* gene. The effectiveness of PCR-RT with primers for the studied genes reached 95–96%.

Table. Primers for RT-PCR.

gene	5'-3'-sequence	coding protein	function of coding protein
SUVH1	CTCTTCCTCTCCCAATCTCAGAC AAAAGGTGAGGGCTGTGGAG	Histone-lysine N-methyltransferase, H3 lysine-9 specific SUVH1	Methylation of H3 lysine 9
CLF	TCAGCGCCGAGTGTAATCTT GTTCCACTCAGATTTGGGCAT	Histone-lysine N-methyltransferase, CLF-like	Methylation of H3 lysine 27
EZA1	TCGGGTTTCATGTCACAGTCA AGATTCAGCGGAAACGGAGG	Histone-lysine N-methyltransferase, EZA1-like	Methylation of H3 lysine 27
SUVR1	TGCTACATCTGAGAGTCTGGG GAAAGGATGGCGGGCTTTTG	Histone-lysine N-methyltransferase, SUVR1	Probably inactive methyltransferase
SUVR3	CACATGCCTCCGAAGCTGAA CCCTTCCAGAATGTGCTTCAAT	Histone-lysine N-methyltransferase, SUVR3-like	Methylation of H3 lysine 9
ATXR4	AGGGAACACACTCAACTCAG AAGCCCTCTGGGATTTGTCG	Histone-lysine N-methyltransferase, ATXR4-like	Methylation of H3 lysine 4
ASHH3	TGCTTCTCCGGTAATCGCTG AGCCAAAAGTATCTGCACACT	Histone-lysine N-methyltransferase, ASHH3	Methylation of H3 lysine 36

2.11. Statistical processing of results

The arithmetic mean values were calculated by the formula: : $M_x = \Sigma X_i/n$. Standard deviations: $\sigma_x = \sqrt{D_x} = \sqrt{\Sigma(X_i - M_x)^2 / n-1}$, where : D_x is the dispersion.

3. Results and discussions

Peptide AEDL at a concentration of 10^{-7} M in the medium was shown to stimulate callusogenesis, increasing the mass of tobacco calluses and enhancing leaf formation [20]. We found here that the total number of regenerants per explant increased in the presence of the peptide, and the mass of regenerants from callus tissue of cotyledonary tobacco leaves increased by approximately 80% compared to the control (Figure 1). Additionally, regenerants with large, square leaf plates were observed. In tobacco regenerants grown on medium containing peptide AEDL, leaf formation began on days 11–12 compared to days 14–15 in control plants. These results indicate that AEDL affects cell differentiation and tissue morphogenesis in tobacco.

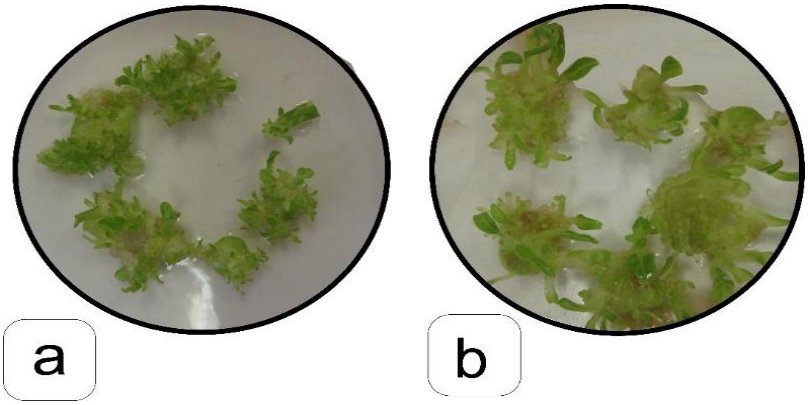

Figure 1. Callus of *Nicotiana tabacum* grown without (a) and with AEDL (b).

Mesophyll cells of developing leaves from tobacco regenerants had large, round nuclei containing a nucleolus, nucleoloplasm, and osmiophil fragments of condensed chromatin (Figure 2a, e). The cytoplasm contained well-developed chloroplasts (Figure 2b, e), and the vacuoles were not fully formed and fused and had not pushed the organelles to the cell periphery, as is typically observed in mature tissues. A high ratio of decondensed to condensed chromatin is detected in young tissues that exhibit high mitotic activity. In this study, we detected condensed chromatin in both the nucleoplasm and near the nuclear membrane (Figure 2a); 10% more cells contained decondensed as compared to condensed chromatin in their nuclei. Treatment with peptide AEDL altered the structural organization of nuclei, as evidenced by the appearance of invaginations and the reduced size and number of condensed chromatin clusters (Figure 2d). A quantitative analysis revealed that the amount of condensed and decondensed chromatin was 25% lower and 75% higher, respectively, in the presence of peptide AEDL in mesophyll cells of developing regenerant leaves (Figure 2c, f).

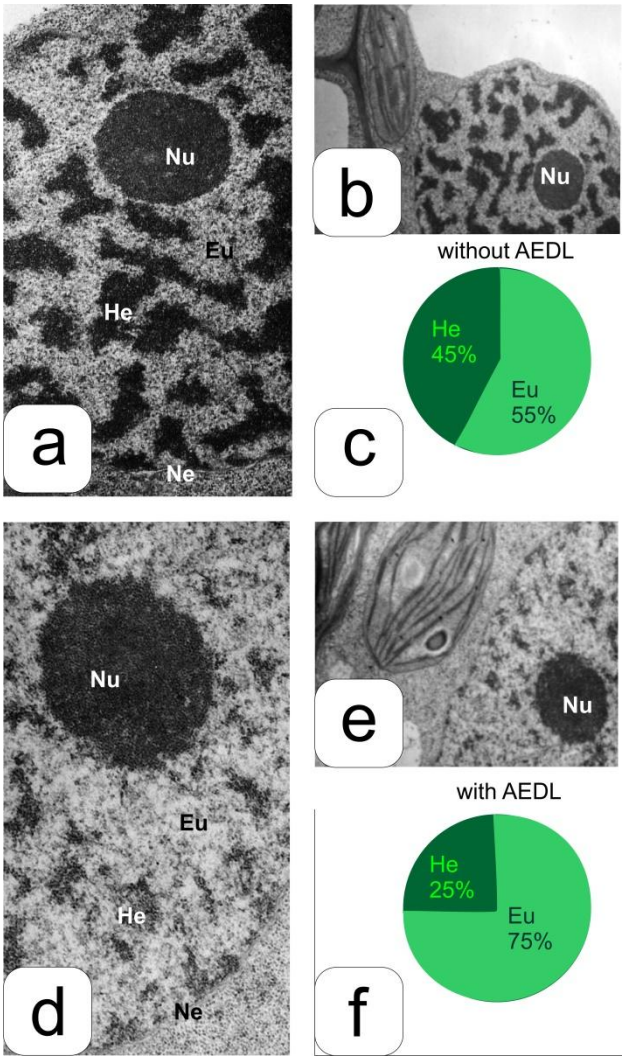

Figure 2. The chromatin ultrastructure of tobacco regenerants grown on MS medium without and in the presence of AEDL. a-Fragment of the nucleus with the nucleolus (control); b-interphase mesophyll cells (control); c-histogram of the ratio of He-condensed and Eu-dispersed chromatin (control); Ne-nucleus envelope; Nu-nucleolus; d-Fragment of the nucleus with the nucleolus (peptide); e-interphase mesophyll cells (peptide); f-a histogram of the ratio of He-condensed and Eu-dispersed chromatin (peptide).

It is known that the rapid dynamics of chromatin condensation as change signify epigenetic interactions and structures can be inherited through cell division. Data also suggest that the assembly of 3D domains in the nucleus with different chromatin morphology, rather than higher-order folding, determines the global accessibility and activity genes [26]. The above results suggest that peptide AEDL alters the organization of nuclei and chromatin, leading to changes in the expression of genes related to development and differentiation. Chromatin decondensation can be attributable to changes in histone modification. It has been suggested that the peptide AEDL modulates gene expression by binding to regulatory proteins. To investigate this possibility, we examined the expression of histone methyltransferase genes. Methylation of Lys residues in the tail of histone H3 by histone Lys

methyltransferases alters chromatin state and gene expression [27]. Most of them contain an evolutionarily conserved SET domain, which is responsible for the activity of methyltransferases [28], which has a length of approximately 130 amino acids and forms a nodular structure that serves as a catalytic center in SET domain group (SDG) histone methyltransferases [29].

The first mammalian lysine histone methyltransferases that were characterized were the homologs of Drosophila SU(VAR) 3–9 and Schizosaccharomyces pombe R4 [30]. The plant homolog, of SU(VAR) 3–9, SUVH, is a heterochromatin-specific H3K9 histone methyltransferase [31]. Although SUVR and SUVH have similar specificity, they are distinguished by the fact that the former is mainly localized in the nucleolus or nuclear bodies and regulate non-condensed euchromatin, whereas the latter associates with and is involved in the silencing of heterochromatin genes [32,33]. SUVR4 represses rDNA gene clusters in the decondensed part of the nucleolus through H3K9 dimethylation [34].

The relative expression level of the SUVH gene decreased in the presence of peptide AEDL (Figure 3). Given that H3K9 lysine methylation is associated with heterochromatin, downregulation of SUVH is associated with an increase in euchromatin and the activation of specific genes. A similar trend was observed with EZA1, another histone methyltransferase.

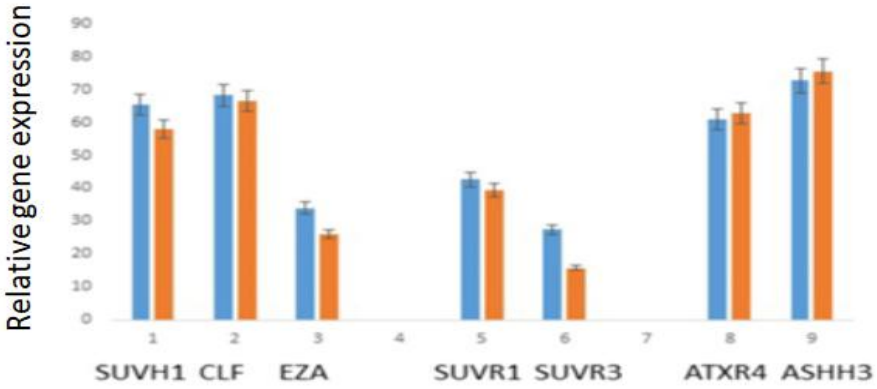

Figure 3. Relative gene expression of different histone methyltransferase families with a SET domain. Blue-cDNA from control tobacco regenerants and orange–from regenerants grown in the presence of the peptide AEDL.

E(Z) containing polycomb repressive complex 2 as a catalytic subunit methylates the lysine residues of histone H3 at position K27 [35], which is also associated with heterochromatin. E(Z) methyltransferases have a broader substrate specificity than SUVH as they also methylate H3K9.

CURLY LEAF (CLF) is one of the main methyltransferases catalyzing the trimethylation of histone H3 lysine 27 (H3K27me3) and plays a significant role in plant growth and development [36]. In Arabidopsis, CLF represses the transcription of AGAMOUS and SHOOT MERISTEMLESS, two genes that determine leaf and flower morphology [37] as well as that of *WUSCHEL* expressed in flower stem cells [38]; it also maintains root meristem activity by inhibiting the expression of PICKLE, a chromatin-remodeling protein [39]. We found that peptide AEDL had little effect on the expression of CLF; however, it increased the level of genes of the ATXR and ASH families encoding

lysine H3K4 and lysine H3K36 methyltransferases, respectively (Figure 3), which are associated with activation of euchromatin. ASH methylates H3K36 and H3K27. The former is largely associated with euchromatin in eukaryotes [40] and is directly related to the elongation activity of RNA polymerase II [41]. Thus, H3K36 methylation is considered an indicator of active chromatin. Trimethylation of H3K36 or di- and trimethylation of H3K27 and H3K9 on the same histone tail is rare; methylation of one lysine residue can inhibit that of a second residue [42]. There are five SDG proteins in Arabidopsis (ATX1–5), which are homologs of eukaryotic Trithorax proteins [43]. ATX1 is involved in H3K4 trimethylation and is necessary for root, leaf, and flower development as well as for the transcriptional regulation of stress response genes [44]. In the presence of AEDL peptide, ATXR family genes encoding lysine H3K4 methyltransferases were upregulated along with ASH family genes, although the increase was non-significant, implying that the observed chromatin decondensation was caused by a mechanism other than activation or inactivation of histone methyltransferase genes.

The histones molecule consists of three parts: they have N and -, C-ends, as well as a highly conserved hydrophobic globular region. The globular part is hydrophobic and represents the most conservative part of the molecule in all histones [45]. The C-terminal domain of histones determines chromatin packaging in vivo [46]. The observed chromatin decondensation in tobacco regenerants in the presence of peptide AEDL may be explained by the binding of the peptide to histone tails and the consequent modification of chromatin structure.

Tobacco histone H1 has several isoforms that were well separated by sodium dodecyl sulfate polyacrylamide gel electrophoresis (SDS-PAGE), with an apparent molecular weight of 35–45 kDa (Figure 4). The isoforms differ in terms of amino acid composition, temporal expression pattern, and degree of post-translational modification [47] and play distinct roles in the organization of chromatin structure. The H1/1 subfraction differs from other subfractions in size and amino acid sequence. Histone H1 in plants and animals have a similar structure, with a conserved central hydrophobic globular domain and positively charged N and C termini [47]. The histones of tobacco appeared different from those of animals by SDS-PAGE (Figure 4). The arginine-rich histones H3 and H4 have near-identical sequences in higher organisms [45] and those from tobacco and animals show similar electrophoretic mobility. Bands corresponding to histones H2A and H2B, which exhibit greater sequence variability, were visible above the H3 band (Figure 4).

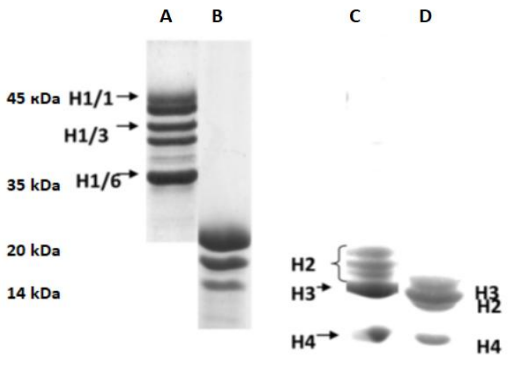

Figure 4. SDS-electrophoresis of histones H1 from Nicotiana tabacum (A) and H1 from rat (B) and of core histones from Nicotiana tabacum (C), from rat (D).

The interaction between histones H1/1 and H3 and peptide AEDL was investigated by fluorescence spectroscopy. Histones were first treated with demethylase to remove methyl groups, which was confirmed by mass spectroscopy. The conjugation of the fluorescent probe fluorescein isothiocyanate (FITC) to histones enables the visualization of protein–protein interactions with greater sensitivity than conventional fluorescence quenching methods. FITC binds to α-amino groups in proteins and preferentially modifies N-terminal amino acids [23]. The position of the fluorescent probe in histones H1/1 and H3 was determined by mass spectrometry after isolation of flurolabel tryptic peptides on HPLC. FITC-labeled histones were excited with a wavelength of 413 nm and emission was recorded in the range of 480 to 580 nm (Figure 5). The maximum observed fluorescence of all FITC-labeled histones was at around 515 nm, suggesting that the microenvironment of the fluorescent probe was similar for these molecules. This allowed us to compare the effects of peptide AEDL on the microenvironment of the fluorophore in histones using the same concentration of FITC–histones in all experiments.

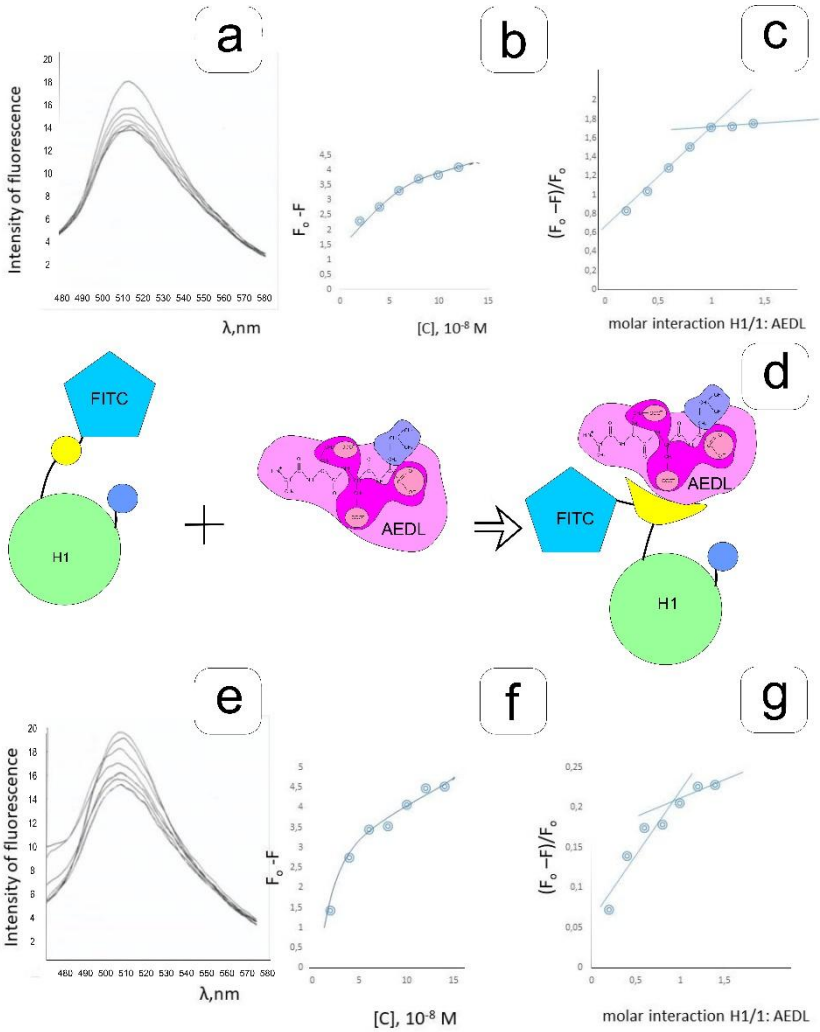

Figure 5. Interaction of AEDL with histone H1/1 (a,b,c) and its complex with DNA (e,f,g). d–scheme binding peptide with FITC-label histone H1/1. The yellow domain-N end of histones, the blue domain-C end of histones.

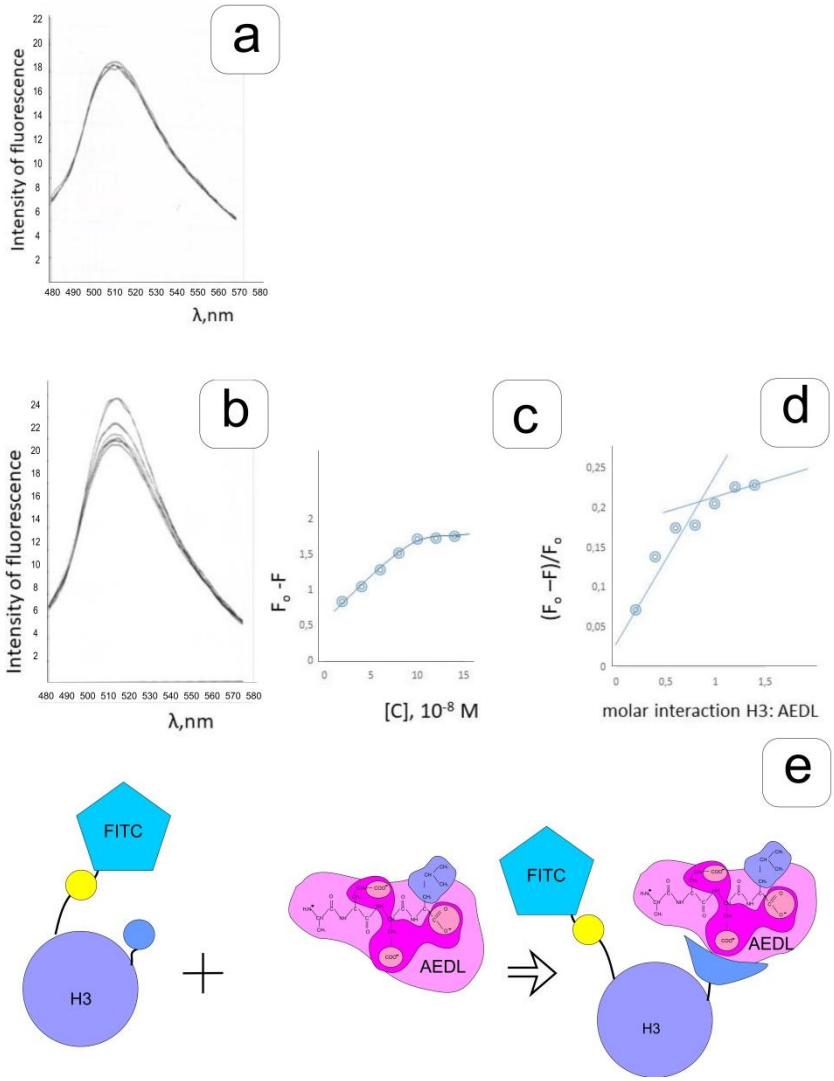

Figure 6. Interaction AEDL with histone H3 (a) and its complex with DNA (b,c,d). e – scheme binding peptide with FITC-label histone H3. The yellow domain-N end of histones, the blue domain-C end of histones.

Emission spectra of FITC–histone H1/1 in the absence and presence of different concentrations of peptide AEDL are shown in Figure 5. At increasing peptide concentrations, the fluorescence intensity of FITC–histone H1/1 was gradually quenched. Static quenching of histone H1/1 fluorescence during the formation of the histone H1/1–peptide complex can be described by the Stern–Volmer equation [24,48]. The dependence of (Fo−F) on peptide concentration was non-linear, indicating that saturation occurred in the binding of histone H1/1 to AEDL. A single site in histone H1/1 was found to bind to the peptide. As fluorescence quenching occurred during titration of the FITC-labeled histone H1/1with peptide AEDL, the latter was presumed to bind to the N terminus of the protein. The binding constant was higher for the binding of AEDL peptide to a histone H1/1-DNA complex than to an isolated histone; the molar ratio of histone H1/1-DNA: AEDL was determined to be 1: 1 (Figure 5). In contrast, no fluorescence quenching was observed upon titration

of FITC-histone H3 with the peptide AEDL (Figure 6); this may be explained by the fact that the negatively charged AEDL did not bind to lysine residues of histone H3, although the N and C termini of histones are unstructured and thus accessible for binding. Binding of the peptide to C-terminal lysine residues (eg, K27 or K36) would not affect the fluorophore located at the N terminus. In the complex of histone H3 with DNA, the N and C termini of the histone are brought closer together. Indeed, peptide titration of the complex was accompanied by fluorescence quenching (Figure 6). The dependence of (Fo−F)/Fo on the molar ratio of histone H3-DNA: peptide showed is one binding site.

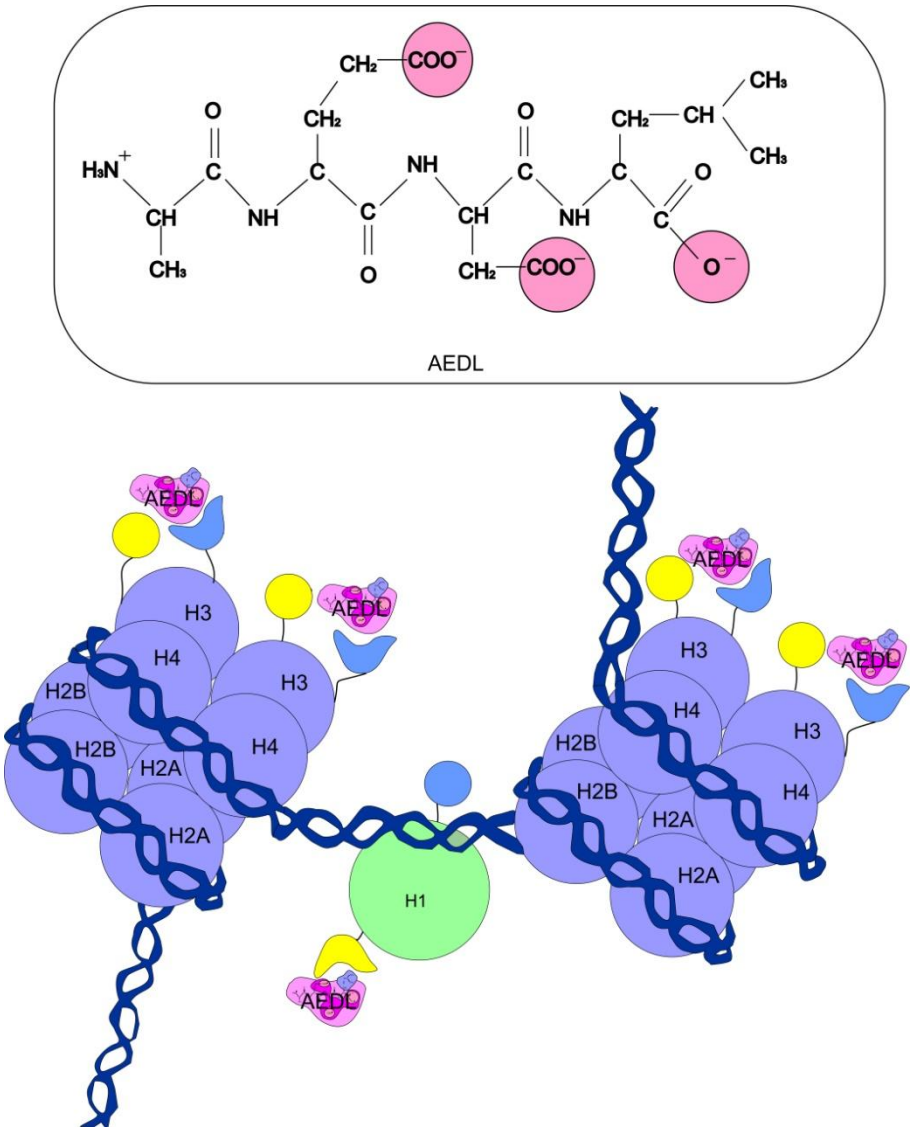

Figure 7. Scheme interaction peptide AEDL with N- terminal lysine residue histone H1 and C-terminal lysine K36 histone H3. The yellow domain-N end of histones, the blue domain-C end of histones.

4. Conclusions

AEDL is a negatively charged peptide and is likely to target positively charged amino acid residues in histones, and these are primarily lysine residues. According to microscopy data, tobacco regenerants grown in the presence of the peptide AEDL exhibit chromatin decondensation as compared to control regenerants, i.e. heterochromatin (transcriptionally inactive structure) is transformed into euchromatin (transcriptionally active structure). We suggest that this effect is mainly due to the fact that peptide AEDL binds to the C-terminus of histone H3 through the lysine residue at position 36 and to the N-terminal lysine of the linker histone H1 (Figure 7).

Conflict of interest

All authors declare no conflicts of interest in this paper.

Acknowledgments

The authors thank for technical support the center scientific equipment of All-Russian Research Institute of Agricultural Biotechnology, are grateful to Khavinson V.Kh. for peptide AEDL synthesis, and to Dilovarova T.A. for tobacco callus.

The study performed in the framework of the Russian state assignment AAA-A1170912-8 and partially RFBR № 18-016-00150.

References

1. Chen DH, Huang Y, Jiang C, et al. (2018) Chromatin-based regulation of plant root development. *Front Plant Sci* 9: 1509.
2. Luger K, Dechassa ML, Tremethick DJ (2012) New insights into nucleosome and chromatin structure: an ordered state or a disordered affair? *Nat Rev Mol Cell Bio* 13: 436–447.
3. Turner BM (2002) Cellular memory and the histone code. *Cell* 111: 285–291.
4. Bannister AJ, Kouzarides T (2011) Regulation of chromatin by histone modifications. *Cell Res* 21: 381–395.
5. Wang N, Liu C (2019) Implications of liquid-liquid phase separation in plant chromatin organization and transcriptional control. *Curr Opin Genet Dev* 55: 59–65.
6. Minard ME, Jain AK, Barton MC (2009) Analysis of epigenetic alterations to chromatin during development. *Genesis* 47: 559–572.
7. Fischle W, Wang Y, Allis CD (2003) Histone and chromatin cross-talk. *Curr Opin Cell Biol* 15: 172–183.
8. Zhang K, Sridhar VV, Zhu J, et al. (2007) Distinctive core histone post-translational modification patterns in Arabidopsis thaliana. *Plos One* 2: 1210.
9. Lippman Z, Gendrel AV, Black M, et al. (2004) Role of transposable elements in heterochromatin and epigenetic control. *Nature* 430: 471–476.
10. Zhang X (2008) The epigenetic landscape of plants. *Science* 320: 489–492.
11. Luger K, Mäder AW, Richmond RK, et al. (1997) Crystal structure of the nucleosome core particle at 2.8 Å resolution. *Nature* 389: 251–260.

12. Kalashnikova AA, Porter-Goff ME, Muthurajan UM, et al. (2013) The role of the nucleosome acidic patch in modulating higher order chromatin structure. *J R Soc Interface* 10: 20121022.
13. McGinty RK, Tan S (2015) Nucleosome structure and function. *Chem Rev* 115: 2255–2273.
14. Grossniklaus U, Vielle-Calzada JP, Hoeppner MA, et al. (1998) Maternal control of embryogenesis by MEDEA, a polycomb group gene in Arabidopsis. *Science* 280: 446–450.
15. Alvarez-Venegas R, Pien S, Sadder M, et al. (2003) ATX-1 an *Arabidopsis* homolog of trithorax, activates flower homeotic genes. *Curr Biol* 13: 627–637.
16. Zhao Z, Yu Y, Meyer D, et al. (2005) Prevention of early flowering by expression of FLOWERING LOCUS C requires methylation of histone H3 K36. *Nat Cell Biol* 7: 1256–1260.
17. Fang Q, Chen P, Wang M, et al. (2016) Human cytomegavirus IE1 protein alters the higher order chromatin structure by targeting the acidic patch of the nucleosome. *eLife* 5: e11911.
18. Tavormina P, De Coninck B, Nikonorova N, et al. (2015) The plant peptidome: an expanding repertoire of structural features and biological functions. *Plant Cell* 27: 2095–2118.
19. Khavinson V, Popovich I (2017) Short peptides regulate gene expression, protein synthesis and enhance life span. *Anti-aging Drugs* 496–513.
20. Fedoreyeva LI, Dilovarova TA, Ashapkin VV, et al. (2017) Short exogenous peptides regulate expression of CLE, KNOX1 and GRF family genes in Nicotiana tabacum. *Biochemistry (Moscow)* 82: 521–528.
21. Khavinson VK, Lezhava TA, Malinin VV (2004) Effects of short peptides on lymphocyte chromatin in senile subjects. *B Exp Biol Med* 137: 78–81.
22. Hieb AR, D'Arcy S, Kramer MA, et al. (2012) Fluorescence strategies for high-throughput quantification of protein interactions. *Nucleic Acids Res* 40: e33.
23. Castell JV, Pestaña A, Castro R, et al. (1978) Fluorometric assays in the study of nucleic acid-protein interactions: II. The use of fluorescamine as a reagent for proteins. *Anal Biochem* 90: 551–560.
24. Lakowicz JR, Weber G (1973) Quenching of fluorescence by oxygen. Probe for structural fluctuations in macromolecules. *Biochemistry* 12: 4161–4170.
25. Xie MX, Long M, Liu Y, et al. (2006) Characterization of the interaction between human serum albumin and morin. *BBA-Gen Subjects* 1760: 1184–1191.
26. Ou HD, Phan S, Deerinck TJ, et al. (2017) ChromEMT: Visualizing 3D chromatin structure and compaction in interphase and mitotic cells. *Science* 357: eaag0025.
27. Thorstensen T, Grini PE, Aalen RB (2011) SET domain proteins in plant development. *BBA-GENE Regul MechE* 1809: 407–420.
28. Baumbusch LO, Thorstensen T, Krauss V, et al. (2001) The Arabidopsis thaliana genome contains at least 29 active genes encoding SET domain proteins that can be assigned to four evolutionarily conserved classes. *Nucleic Acids Res* 29: 4319–4333.
29. Qian C, Zhou MM (2006) SET domain protein lysine methyltransferases: Structure, specificity and catalysis. *Cell Mol Life Sci* 63: 2755–2763.
30. Tschiersch B, Hofmann A, Krauss V, et al. (1994) The protein encoded by the Drosophila position-effect variegation suppressor gene Su(var)3–9 combines domains of antagonistic regulators of homeotic gene complexes. *EMBO J* 13: 3822–3831.
31. Rea S, Eisenhaber F, O'Carroll D, et al. (2000) Regulation chromatin structure by site-specific histone H3 methyltransferases. *Nature* 406: 593–599.

32. Jackson JP, Johnson L, Jasencakova Z, et al. (2004) Dimethylation of histone H3 lysine 9 is a critical mark for DNA methylation and gene silencing in Arabidopsis thaliana. *Chromosoma* 112: 308–315.
33. Jasencakova Z, Soppe WJJ, Meister A, et al. (2003) Histone modifications in Arabidopsis–high methylation of H3 lysine 9 is dispensable for constitutive heterochromatin. *Plant J* 33: 471–480.
34. Neves N, Delgado M, Silva M, et al. (2005) Ribosomal DNA heterochromatin in plants. *Cytogenet genome res* 109: 104–111.
35. Frapporti A, Pina CM, Arnaiz O, et al. (2019) The Polycomb protein Ezl1 mediates H3K9 and H3K27 methylation to repress transposableelements in Paramecium. *Nat Commun* 10: 1–15.
36. Shu J, Chen C, Thapa RK, et al. (2019) Genome-wide occupancy of histone H3K27 methyltransferases CURLY LEAF and SWINGER in Arabidopsis seedlings. *Plant Direct* 3: e00100.
37. Müller-Xing R, Clarenz O, Pokorny L, et al. (2014) Polycomb-group proteins and FLOWERING LOCUS T maintain commitment to flowering in Arabidopsis thaliana. *Plant Cell* 26: 2457–2471.
38. Liu X, Kim YJ, Müller R, et al. (2011) AGAMOUS terminates floral stem cell maintenance in Arabidopsis by directly repressing WUSCHEL through recruitment of Polycomb group proteins. *Plant Cell* 23: 3654–3670.
39. Aichinger E, Villar CBR, Di Mambro R, et al. (2011) The CHD3 chromatin remodeler PICKLE and Polycomb group proteins antagonistically regulate meristem activity in the Arabidopsis root. *Plant Cell* 23: 1047–1060.
40. Ho JWK, Jung YL, Liu T, et al. (2014) Comparative analysis of metazoan chromatin organization. *Nature* 512: 449–452.
41. Kizer KO, Phatnani HP, Shibata Y, et al. (2005) A novel domain in Set2 mediates RNA polymerase II interaction and couples histone H3 K36 methylation with transcript elongation. *Mol Cell Biol* 25: 3305–3316.
42. Schmitges FW, Prusty AB, Faty M, et al. (2011) Histone methylation by PRC2 is inhibited by active chromatin marks. *Mol Cell* 42: 330–341.
43. Schuettengruber B, Martinez AM, Iovino N, et al. (2011) Trithorax group proteins: Switching genes on and keeping them active. *Nat Rev Mol Cell Bio* 12: 799–814.
44. Napsucialy-Mendivil S, Alvarez-Venegas R, Shishkova S, et al. (2014) Arabidopsis homolog of trithorax1 (ATX1) is required for cell production, patterning, and morphogenesis in root development. *J Exp Bot* 65: 6373–6384.
45. GANTT JS, Lenvik TR (1991) Arabidopsis thaliana H1 histones. Analysis of two members of a small gene family. *Eur J Biochem* 202: 1029–1039.
46. Bednar J, Horowitz RA, Grigoryev SA, et al. (1998) Nucleosomes, linker DNA, and linker histone form a unique structural motif that directs the higher-order folding and compaction of chromatin. *P Natl Acad Sci* 95: 14173–14178.
47. Happel N, Doenecke D (2009) Histone H1 and its isoforms. Contribution to chromatin structure and function. *Gene* 431: 1–12.
48. Favicchio R, Dragan AI, Kneale GG, et al. (2009) Fluorescence spectroscopy and anisotropy in the analysis of DNA-protein interactions. *Methods in Mol Biol* 543: 589–611.